PHENOMENOLOGICAL AND MICROSCOPIC OPTICAL-MODEL DESCRIPTIONS OF 99 MeV ^{6}Li SCATTERING

P. Schwandt, W. Ploughe,[*] F.D. Becchetti,[**] J. Jänecke,[**] W.W. Jacobs, P.P. Singh,
M.D. Kaitchuck, J. Meek, and F. Petrovich[***]

The optical model (OM) analysis of the ^{6}Li elastic cross sections$^{1)}$ for ^{12}C, ^{28}Si, ^{40}Ca, ^{58}Ni, ^{90}Zr, and ^{208}Pb at 99 MeV bombarding energy begun a year ago has been completed. The angular distributions shown in Figure 1 were analyzed in terms of a phenomenological 6-parameter, complex, central potential with Woods-Saxon formfactors. Excellent fits to the data were obtained (solid curves in Figure 1) with an essentially common parametrization of the real potential for all nuclei, namely

$$V = 94 \text{ MeV}, \; r_o = 1.30 \text{ fm}, \; a_o \simeq 0.85 \text{ fm}.$$

All potential parameters are listed in Table 1, along with the volume integrals per nucleon of real and imaginary potentials, the real potential rms radius, and the calculated reaction cross section. For the target nuclei heavier than ^{12}C, the average geometrical parameters of the imaginary potential are well represented by the relations

$$r_w \simeq 2.19 - .115 \, A^{1/3} \quad \text{(fm)}$$

$$a_w \simeq 0.66 + .029 \, A^{1/3} \quad \text{(fm)}$$

where A is the target mass number, while the imaginary strength appears to be essentially A-independent, $W \simeq 21 \pm 2$ MeV.

We find that even at this elevated energy ^{6}Li scattering is still sensitive primarily to the nuclear potential in the surface region only, largely beyond the half-density point. This is illustrated in Figure 2 by the results of a notch-perturbation test in which a localized "notch" is introduced in the real potential at a radius R_{notch} which is then moved across a radial region of interest in order to explore the sensitivity of the fit to the data (as expressed by the usual objective quality-of-fit criterion χ^2) to a given potential region. The arrows in Figure 2 indicate the location of the half-maximum radius of the real potential for each of the three nuclei.

We have also explored the discrete potential ambiguities universally encountered for moderately-to-strongly absorbed projectiles at lower energies and found that 100 MeV ^{6}Li scattering can be adequately described by a variety of real potentials differing in well depth V by ∿ 50 MeV, from V ∿ 100 to V ∿ 300

Table 1.

Target	V	r_o	a_o	W	r_w	a_w	$J_R/6A$	$J_I/6A$	$\langle r^2 \rangle_R^{1/2}$	σ_R
^{12}C	94.0	1.30	.808	40.5	1.261	1.155	250	148	3.79	1470
^{28}Si	94.0	1.30	.839	21.9	1.849	.751	209	114	4.37	1670
^{40}Ca	94.0	1.30	.875	18.6	1.880	.715	199	97	4.74	1890
^{58}Ni	94.0	1.30	.865	21.1	1.729	.769	186	86	5.05	2085
^{90}Zr	94.0	1.30	.845	20.5	1.685	.805	174	76	5.50	2460
^{208}Pb	94.0	1.30	.826	23.5	1.518	.821	160	62	6.71	2875

(All potential strengths in MeV, geometry parameters in fm, volume integrals in MeV-fm , rms radii in fm, reaction cross section in mb.)

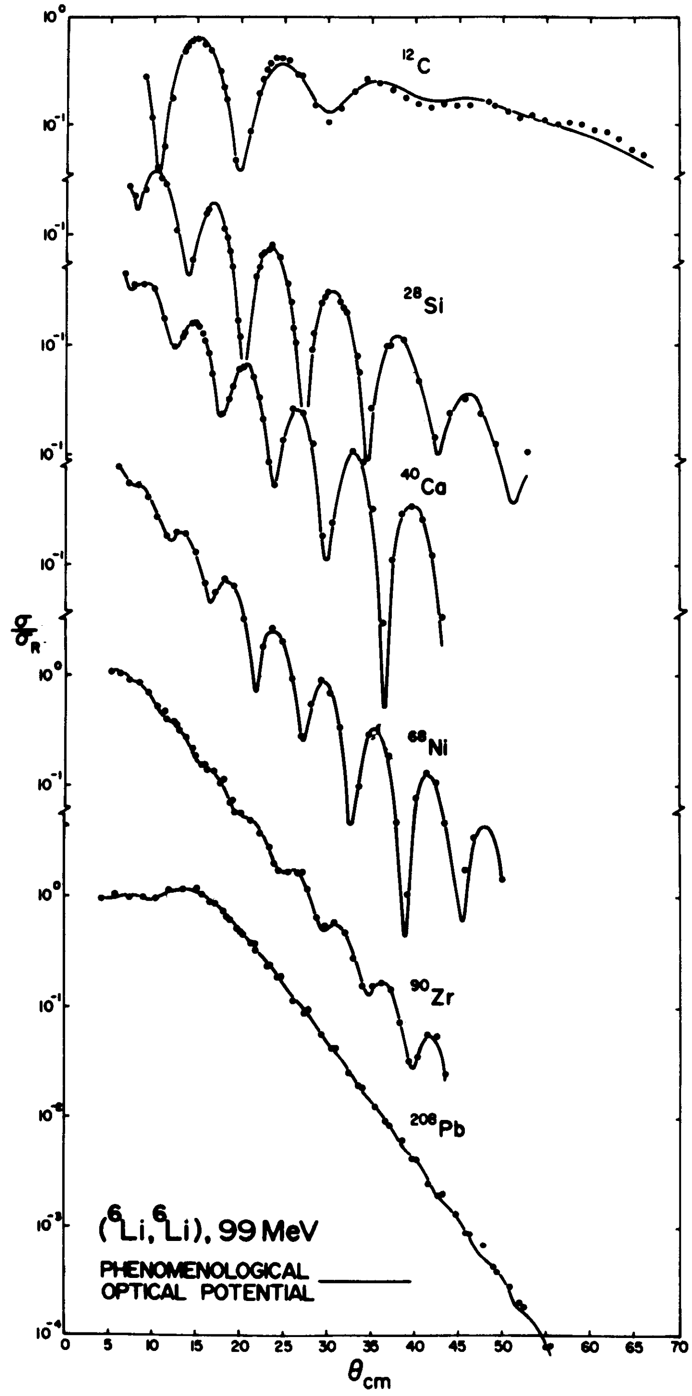

Figure 1.

MeV for A = 28-90, and from V ∿ 50 to V ∿ 200 MeV for ^{208}Pb. This ambiguity is illustrated in Figure 3 for the case ^{58}Ni which is representative of the behavior for medium mass nuclei. (The solid curve presents the χ^2-minima as function of V with all other parameters adjusted for a best fit; the dashed curve illustrates the observed continuous V - r_o correlation

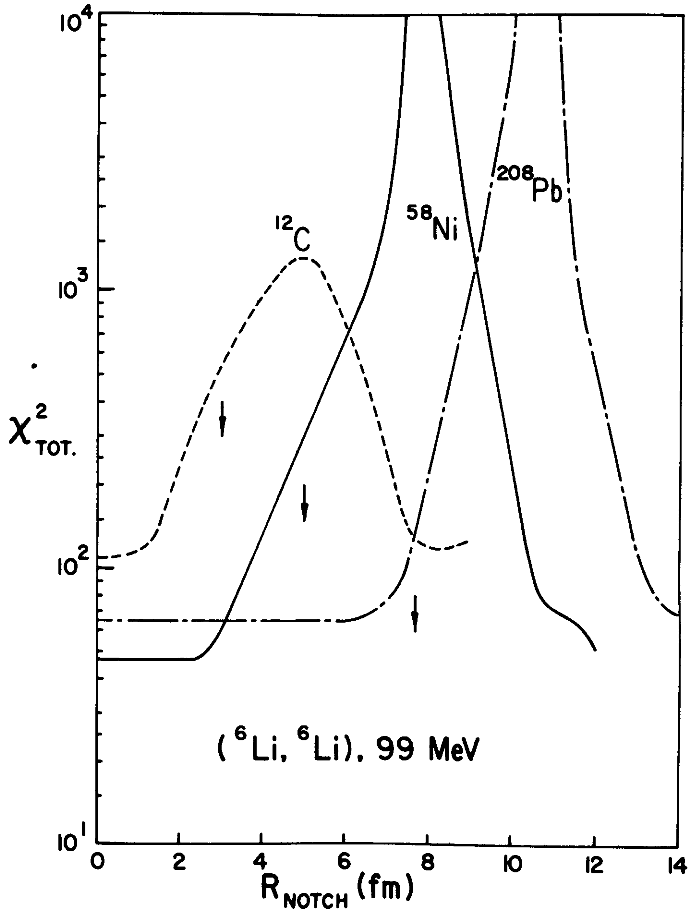

Figure 2.

which may be represented approximately by the relation V r_o^n = const. with n = 5.2.) The best fits to all nuclei indicate a mild preference for the V ∿ 100 or V ∿ 150 MeV members of the discrete potential family. As indicated in the next contribution to this report, higher-energy ^{6}Li scattering appears to select V ∿ 150 MeV as the most likely candidate for the real central strength of the ^{6}Li optical potential with Woods-Saxon formfactors.

As described in last year's report,$^{1)}$ we also attempted to describe the ^{6}Li scattering in a semi-microscopic approach by generating the real optical potential in a (d+α)-cluster folding model. That

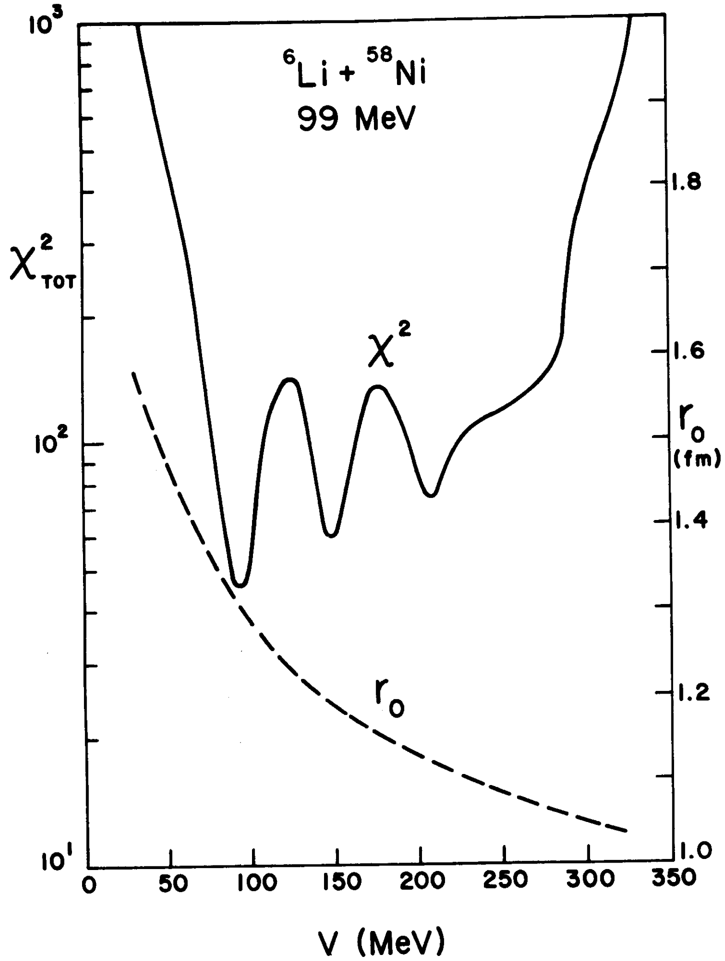

Figure 3.

approach proved successful when the folded potential strength was allowed to be renormalized by a factor of ∿ 0.5. More recently, one of the authors (FP) has generated the ^{6}Li optical potential by means of a double-folding model using a realistic, complex G-matrix for the effective 2-nucleon interaction. Both real and imaginary parts of the ^{6}Li potential were calculated in this manner, with a term $A\delta(r)$ added to the G-matrix used in the absorptive part. Again, in order to fit the 99 MeV ^{6}Li data, both real and imaginary central strengths needed to be renormalized by factors ranging from 0.66 to 0.51. With such renormalization the fits to the experimental data are excellent, as illustrated in Figure 4, with χ^2 values ranging from 0.8 to 4.2 times the χ^2 values obtained

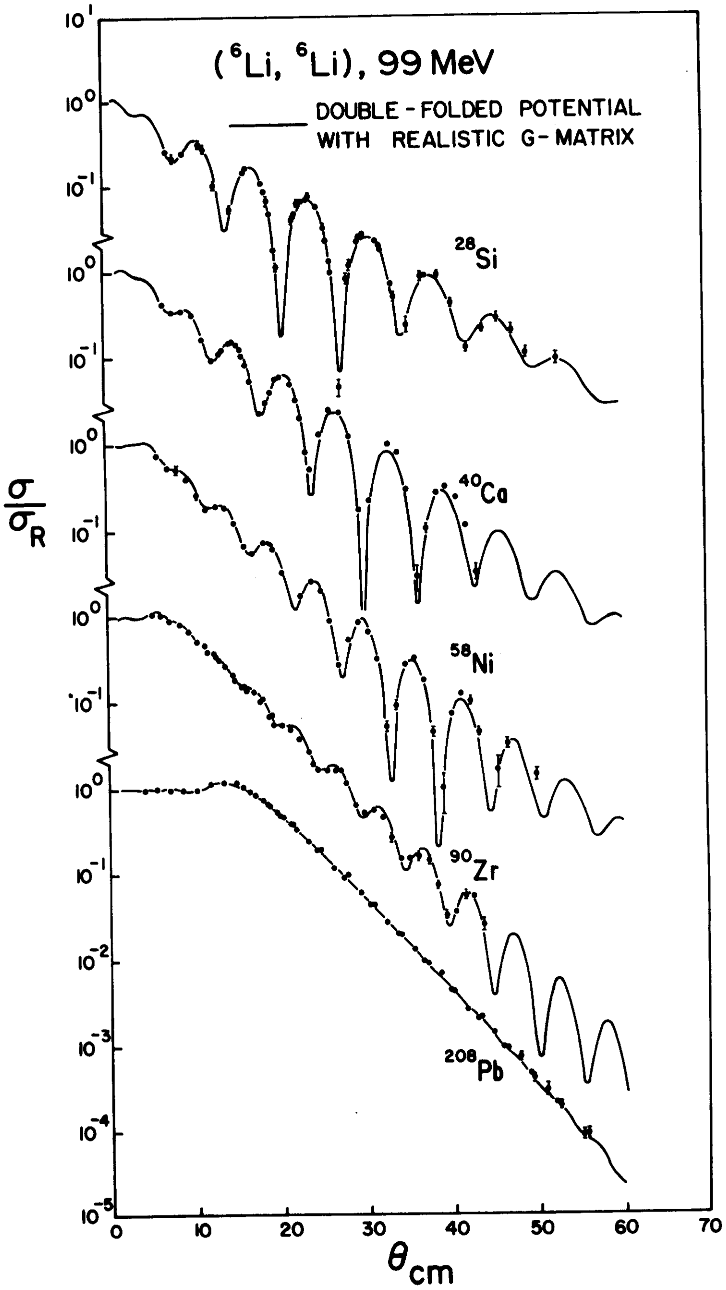

Figure 4.

with the phenomenological OM. Once the reason for the renormalization is understood (its source is not the Pauli principle which reduces the attraction in the nuclear interior while the data requires a factor of 2 reduction in strength in the low-density surface and tail regions of the potential), then the microscopic potential models based on either cluster or 2-nucleon folding may well provide a much less ambiguous and physically more meaningful description of ^{6}Li scattering at medium energies than the phenomenological OM.

[*]Ohio State University, Columbus, OH 43210

[**]University of Michigan, Ann Arbor, MI 48104

[***]Florida State University, Tallahassee, FL 32306

1) P. Schwandt et al., IUCF Techn. and Scient. Report 1977, p. 85; ibid., B.A.P.S. 22, 633 (1977).